BIOCHEMISTRY
including biophysical chemistry & molecular biology

Article

pubs.acs.org/biochemistry

Observation of Two Modes of Inhibition of Human Microsomal Prostaglandin E Synthase 1 by the Cyclopentenone 15-Deoxy-$\Delta^{12,14}$-prostaglandin J_2

Edward B. Prage,[†] Ralf Morgenstern,[§] Per-Johan Jakobsson,[‡] Donald F. Stec,[†] Markus W. Voehler,[†] and Richard N. Armstrong*[,†]

[†]Departments of Chemistry and Biochemistry, Center in Molecular Toxicology, and Vanderbilt Institute of Chemical Biology, Vanderbilt University, Nashville, Tennessee 37232-0146, United States

[‡]Department of Medicine, Rheumatology Unit, Karolinska Institutet, S-171 76 Stockholm, Sweden

[§]Institute of Environmental Medicine, Karolinska Institutet, S-171 77 Stockholm, Sweden

Supporting Information

ABSTRACT: Microsomal prostaglandin E synthase 1 (MPGES1) is an enzyme that produces the pro-inflammatory molecule prostaglandin E_2 (PGE_2). Effective inhibitors of MPGES1 are of considerable pharmacological interest for the selective control of pain, fever, and inflammation. The isoprostane, 15-deoxy-$\Delta^{12,14}$-prostaglandin J_2 (15d-PGJ_2), a naturally occurring degradation product of prostaglandin D_2, is known to have anti-inflammatory properties. In this paper, we demonstrate that 15d-PGJ_2 can inhibit MPGES1 by covalent modification of residue C59 and by noncovalent inhibition through binding at the substrate (PGH_2) binding site. The mechanism of inhibition is dissected by analysis of the native enzyme and the MPGES1 C59A mutant in the presence of glutathione (GSH) and glutathione sulfonate. The location of inhibitor adduction and noncovalent binding was determined by triple mass spectrometry sequencing and with backbone amide H/D exchange mass spectrometry. The kinetics, regiochemistry, and stereochemistry of the spontaneous reaction of GSH with 15d-PGJ_2 were determined. The question of whether the anti-inflammatory properties of 15d-PGJ_2 are due to inhibition of MPGES1 is discussed.

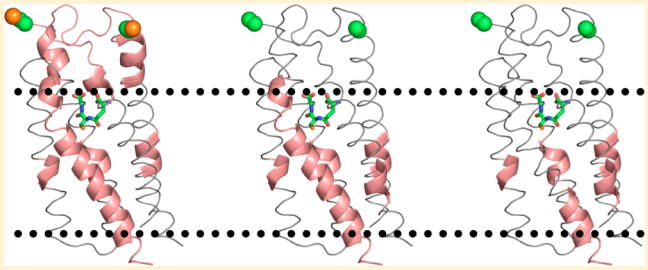

Prostaglandins (PGs) are signaling molecules derived from arachidonic acid (Figure 1) that possess a wide range of biological activities, exerting their functions by binding to G-protein-coupled receptors. For example, prostaglandin E_2 (PGE_2) binds to E-prostanoid (EP) receptors 1−4, eliciting responses involving gastric mucosal integrity, fertility, immune modulation, and inflammation.[1−4] Similarly, prostaglandin D_2 (PGD_2) promotes vasodilation and is also involved in the regulation of body temperature and physiological sleep by binding to D-prostanoid (DP) receptors 1 and 2.[5−7]

Dehydration of PGE_2 and PGD_2 gives rise to a subclass of prostaglandins known as cyclopentenone PGs (cyPGs).[8] One member of this subclass is 15-deoxy-$\Delta^{12,14}$-prostaglandin J_2 (15d-PGJ_2), which arises from the spontaneous dehydration of PGD_2 (Figure 1) initially forming PGJ_2. PGJ_2 then isomerizes to form Δ^{12}-PGJ_2, which, after the spontaneous loss of an additional molecule of water, results in the formation of 15d-PGJ_2.[9] The biological attributes of this particular cyPG are interesting and wide-ranging. Although it has a much lower affinity for its corresponding DP receptors, it has been reported to selectively bind to peroxisome proliferator-activated receptor γ (PPARγ) with an EC_{50} value in the low micromolar range, which may impart the reported anti-inflammatory signaling properties associated with 15d-PGJ_2.[10] For a recent and excellent review of the chemistry and biological activities of 15d-PGJ_2 and other isoprostane eicosanoids, please see the work of Milne et al.[11]

The chemical properties of 15d-PGJ_2 appear to be dominated by the electrophilic α,β-unsaturated carbonyl group on the cyclopentenone ring that results in the formation of adducts with cellular nucleophiles via Michael addition at C-9.[12] The nucleophiles commonly include cysteine-containing molecules, such as glutathione and cellular proteins.[13] In principle, 1,4-addition at C-13 or 1,6-addition at C-15 could also occur, but they have not been observed. For a comprehensive review of the interaction of electrophilic lipids with cellular nucleophiles, particularly proteins, please see the work of Stamatakis and Perez-Sala.[14]

The pro-inflammatory signaling molecule PGE_2 is synthesized in a glutathione (GSH)-dependent isomerization reaction catalyzed by microsomal prostaglandin E synthase 1 (MPGES1) as shown in Figure 1. PGE_2 is a well-known

Received: December 30, 2011
Revised: February 16, 2012
Published: February 23, 2012

   dx.doi.org/10.1021/bi2019332 | *Biochemistry* 2012, 51, 2348−2356

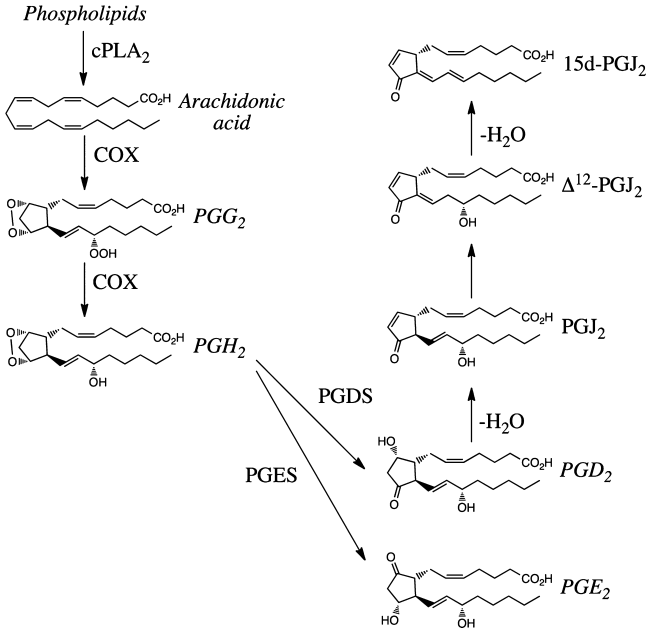

Figure 1. Pathway for the enzyme-catalyzed formation of PGE_2 and PGD_2 from PGH_2. The formation of PGJ_2, Δ^{12}-PGJ_2, and 15d-PGJ_2 from PGD_2 is thought to occur through a series of spontaneous reactions.

mediator of pain, fever, and inflammation.[15] Most current anti-inflammatory therapies rely on the inhibition of cyclooxygenase (COX) (see Figure 1) by nonsteroidal anti-inflammatory drugs (NSAIDs) or COX-2 selective inhibitors (coxibs), which decrease the concentration of PGH_2 and hence that of PGE_2. However, these treatments, which alter the concentrations of several prostaglandins and thromboxanes, can have adverse cardiovascular effects.[16] The MPGES1 enzyme, which is induced under inflammatory conditions, is functionally coupled to COX-2 and represents an alternative therapeutic target for the treatment of inflammatory diseases.[17,18] As a consequence, MPGES1 is currently under investigation as a target for direct therapeutic intervention.

One known naturally occurring inhibitor of MPGES1 is 15d-PGJ_2. In 2002, Quraishi et al.[19] reported that MPGES1 was inhibited by 15d-PGJ_2 with an IC_{50} value of 0.3 μM. In addition, the authors noted that increasing the substrate concentration (PGH_2) failed to rescue enzyme activity, suggesting that the inhibition is not simply competitive but might involve allosteric binding of the inhibitor or the formation of a covalent adduct. The inhibition of MPGES1 is another possible route for the observed anti-inflammatory properties of 15d-PGJ_2. The exact mechanism of inhibition and its physiological relevance have remained an enigma.

The chemical and physical properties of 15d-PGJ_2 raise several very interesting questions about the possible mechanisms of inhibition of MPGES1. Is the enzyme covalently adducted by the inhibitor? Is the enzyme inhibited competitively by 15d-PGJ_2? Is the enzyme inhibited by a GSH adduct of 15d-PGJ_2? Does the enzyme catalyze the addition of GSH to 15d-PGJ_2?

In this paper, we describe a series of biochemical and mass spectrometry (MS) experiments, which indicate that the inhibition of MPGES1 by 15d-PGJ_2 can occur by covalent adduction of the enzyme at C59 with a stoichiometry of one adduct per subunit in the trimer or by simple competitive inhibition of the C59A mutant protein. We demonstrate that the molecular footprints of the two modes of inhibition are quite distinct, as revealed by backbone amide hydrogen/deuterium (H/D) exchange kinetics. The equilibrium constant for the reaction of GSH with 15d-PGJ_2 to form the 9-(*S*-glutathionyl)-15d-PGJ_2 adduct is 3800 M^{-1}. In addition, the enzyme does not appear to catalyze the formation of this adduct. The $NaBH_3CN$-reduced adducts, 9-(*S*-glutathionyl)-11-hydroxy-15d-PGJ_2, are not effective inhibitors of the enzyme. The kinetic and biochemical results suggest that 15d-PGJ_2 is an effective multimode inhibitor of MPGES1 in vitro. The question of whether 15d-PGJ_2 has special significance in vivo, perhaps as an anti-inflammatory molecule, is discussed.

MATERIALS AND METHODS

Materials. Buffer salts and common chemicals were of the highest quality commercially available. Detergents were from Affymetrix Anatrace (Santa Clara, CA). 15d-PGJ_2, PGH_2, and malondialdehyde were obtained from Cayman Chemical (Ann Arbor, MI). The MPGES1 enzyme with GSH or glutathione sulfonate (GSO_3^-) bound was expressed and purified as previously described.[20]

Expression and Purification of the C59A Mutant of MPGES1. The gene encoding the native human MPGES1 enzyme with a C-terminal hexahistidine tag was contained in a pET-21b vector. Via standard polymerase chain reaction, cysteine 59 was mutated to alanine using the forward primer, GGC CCC CAG TAT GCC AGG AGT GAC CCC, and the reverse primer, GGG GTC ACT CCT GGC ATA CTG GGG GCC. The resulting enzyme is hereafter termed MPGES1 C59A. *Escherichia coli* cell culture and enzyme preparation utilizing ultracentrifugation, Ni^{2+} affinity chromatography, and sulfopropyl strong cation exchange chromatography were preformed as previously described[20] with the exception that dithiothreitol (DTT) was not included in either the last chromatography step or the final dialysis. Instead, these buffers were purged with argon.

Preparation of 9-(*S*-Glutathionyl)-11-hydroxy-15d-PGJ_2 and 11-Hydroxy-15d-PGJ_2. The 9-(*S*-glutathionyl)-11-hydroxy-15d-PGJ_2 adduct of 15d-PGJ_2 was prepared by adding 40 μL of a 25 mM solution of 15d-PGJ_2 in DMSO to 160 μL of 6.3 mM GSH in 100 mM KH_2PO_4 (pH 7.0) and incubating the mixture at room temperature for 1 h. The adduct was then reduced by the addition of 10 μL of a 1 M suspension of $NaBH_3CN$ in THF and storage overnight at 4 °C. The reaction mixture was diluted 10-fold in 20 mM Tris (pH 8.0). We purified the product by diethylaminoethyl (DEAE) weak anion exchange chromatography, washed it with 20 mM Tris (pH 8.0), and eluted it with 100 mM KH_2PO_4 (pH 7.5) containing 1 M KCl, 1% glycerol, and 1% CHAPS. The 11-hydroxy-15d-PGJ_2 was prepared as described above without the reaction with GSH.

Preparation of 9-(*S*-Glutathionyl)-15d-PGJ_2. The addition of GSH to 15d-PGJ_2 was initiated by the addition of 1.5 mL of 10 mM GSH in 100 mM KH_2PO_4 (pH 7.0) to 500 μg of 15d-PGJ_2 at 40 °C for 30 min. The reaction was stopped by the addition of 100 μL of 70% H_2SO_4, after which the sample was applied to a 6 cm^3 Oasis HLB solid-phase extraction cartridge that was previously activated with methanol and hydrated with 50 mM ammonium acetate (pH 3). The sample was washed with 50 mM ammonium acetate (pH 3) and eluted with methanol. After evaporation under nitrogen, the sample was

dx.doi.org/10.1021/bi2019332 | *Biochemistry* 2012, 51, 2348−2356

reconstituted in 15% CH_3CN and 0.01% formic acid and stored on dry ice. It was subsequently purified by high-performance liquid chromatography (HPLC), monitoring at 308 nm, using a Beckman 5 μm, 80 Å C18 column (4.6 mm × 25 cm), and eluted at 1 mL/min, with a gradient from 15 to 95% CH_3CN and 0.01% formic acid over a 30 min period. After the 9-(*S*-glutathionyl)-15d-PGJ_2 peak had been collected at approximately 20 min on dry ice, the sample was dried under vacuum and stored desiccated at −20 °C.

Structure of 9-(*S*-Glutathionyl)-11-hydroxy-15d-PGJ_2. The structure of the glutathionyl adduct of 15d-PGJ_2 was determined by LC−MS/MS, as well as by two-dimensional (2D) NMR spectroscopy. For MS analysis, the borohydride-reduced GSH adduct was prepared as described above. In addition, a cysteine adduct was prepared as described above, replacing GSH with equimolar L-cysteine. Analysis was performed by reverse-phase LC−MS/MS, using a Phenomenex Synergi 2.5 μm, Hydro-RP, 100 Å (100 mm × 2.00 mm) C18 column, and eluted at 0.2 mL/min with a gradient from 15 to 95% CH_3CN and 0.01% formic acid over a 30 min period. Ions at m/z 300−1300 were detected on a ThermoFinnigan TSQ triple-quadrupole mass spectrometer using positive electrospray ionization. The PG adduct was identified with a mass corresponding to the monoisotopic mass of GSH or cysteine plus the monoisotopic mass of 15d-PGJ_2, and the site of adduction was determined by MS/MS fragmentation.

The diastereoselectivity of the reaction of GSH with 15d-PGJ_2 was determined by 2D NMR spectroscopy at high field. NMR data were acquired using either a 22.1 T Bruker magnet equipped with a Bruker AV-III console or a 14.9 T Bruker magnet equipped with a Bruker AV-III console. All spectra were acquired in 3 mm NMR tubes using a Bruker 5 mm TCI cryogenically cooled NMR probe. Chemical shifts were referenced internally to CD_3OD (3.30 ppm) or D_2O (4.70 ppm), which also served as the ^2H lock solvents. For one-dimensional (1D) ^1H NMR, typical experimental conditions included 32K data points, a 13 ppm sweep width, a recycle delay of 1.5, and 32 scans. For samples in D_2O, water suppression using presaturation was implemented to reduce the magnitude of the signal of residual H_2O. For 2D $^1H-^1H$ COSY and DQF-COSY, experimental conditions included a 2048 × 512 data matrix, a 13 ppm sweep width, a recycle delay of 1.5, and four scans per increment. The data were processed using a squared sine-bell window function, displayed in either the magnitude mode (COSY) or absolute intensity mode (DQF-COSY). Similar experimental parameters were used to conduct 2D $^1H-^1H$ nuclear Overhauser effect (NOESY) experiments that were acquired with a mixing time of 400 ms. The data were processed using a $\pi/2$-shifted squared sine window function displayed in absolute intensity mode. Multiplicity-edited HSQC experiments were acquired using a 1024 × 256 data matrix, a J(C−H) value of 145 Hz that resulted in a multiplicity selection delay of 34 ms, a recycle delay of 1.5, and 16 scans per increment along with GARP decoupling on ^{13}C during the acquisition time (150 ms). The data were processed using a $\pi/2$-shifted squared sine window function and displayed with CH/CH_3 signals phased positive and CH_2 signals phased negative.

Kinetics of the Spontaneous Reaction of GSH with 15d-PGJ_2. The kinetics of the approach to equilibrium were determined at 25 °C under pseudo-first-order conditions with a fixed 15d-PGJ_2 concentration of 40 μM and a variable excess concentration of GSH ranging between 0.5 and 5.0 mM in 100 mM KH_2PO_4 (pH 7.0). Reactions were initiated by the addition of 10 μL of a 4.0 mM stock solution of 15d-PGJ_2 in 20 mM KH_2PO_4 (pH 7.0) to 990 μL of GSH in the same buffer. The formation of the glutathionyl adduct was observed spectrophotometrically as an exponential decrease in absorbance at 250 nm. The concentration dependence of k_{obs} was used to determine the rate constants for the forward (k_1) and reverse (k_{-1}) reactions from the equation $k_{obs} = k_1[GSH] + k_{-1}$.

In addition, the equilibrium constant for formation (K_f) of 9-(*S*-glutathionyl)-15d-PGJ_2 was calculated by determining the final concentrations of reactants and products at equilibrium at four different initial reactant concentrations. Two reactions were initiated by the addition of 25 μL of a 2 mM 15d-PGJ_2 stock solution in 100 mM KH_2PO_4 (pH 7) to 475 μL of 105 or 211 μM GSH in the same buffer, giving an initial 15d-PGJ_2 concentration of 100 μM and an initial concentration of GSH of 100 or 200 μM, respectively. Two additional reactions were initiated by the addition of 50 μL of the same 15d-PGJ_2 stock solution to 450 μL of 111 or 222 μM GSH, giving a 15d-PGJ_2 concentration of 200 μM and a GSH concentration of 100 or 200 μM, respectively. Each reaction mixture was incubated at 4 °C overnight. After being equilibrated to 22 °C for 1 h, the samples were analyzed by HPLC, monitoring the absorbance at 316 nm, using a Phenomenex Synergi 2.5 μm, Hydro-RP, 100 Å, C18 column (100 mm × 2.00 mm), and eluted at 0.2 mL/min with a gradient from 15 to 95% CH_3CN with 0.05% trichloroacetic acid over a 30 min period.

Enzyme Activity Assays. The catalytic conversion of PGH_2 to PGE_2 was verified by the previously described method,[18] and the detection of PGE_2 by LC−MS/MS was performed as previously published.[21] Reactions were initiated at 0 °C by the addition of 100 μL of a 100 nM enzyme stock solution in reaction buffer [100 mM KH_2PO_4 (pH 7.5) containing 2.5 mM GSH, 1% glycerol, and 1% CHAPS] to 6.7 μL of 75, 150, or 300 μM PGH_2 in acetone. After a 1 min incubation on ice, unreacted PGH_2 decomposed to malondialdehyde (MDA) and 12(*S*)-hydroxy-8,10-*trans*-5-*cis*-heptadecatrienoic acid (12-HHT) by the addition of 400 μL of 25 mM $FeCl_2$ in 50 mM citric acid (pH 3), which included 0.5 μM 11β-PGE_2 as an internal standard. After solid-phase extraction, the resulting prostaglandins were reconstituted in 5% CH_3CN and analyzed by reversed-phase LC−MS/MS, with a Phenomenex Synergi 2.5 μm, Hydro-RP, 100 Å C18 column (100 mm × 2.00 mm), and eluted at a flow rate of 0.2 mL/min with 32% CH_3CN and 0.1% formic acid in water. Single-reaction monitoring (SRM) of the transition from m/z 351 to 271 was utilized for the detection of PGE_2 on a ThermoFinnigan TSQ triple-quadrupole mass spectrometer using negative electrospray ionization. To verify inhibition by 15d-PGJ_2, the procedure was repeated with the enzyme preincubated for 1 h on ice with 100 μM 15d-PGJ_2.

The inhibition of MPGES1 by 15d-PGJ_2 was assessed with a method adapted from a previously described technique.[22] The enzyme, complexed with GSO_3^-, was combined with the inhibitor by addition of 10 μL of solutions of 15d-PGJ_2 ranging in concentration from 0.1 μM to 5 mM in reaction buffer (lacking GSH) to 90 μL of a 1.1 μM enzyme solution in reaction buffer, giving a final enzyme concentration of 1 μM and a final 15d-PGJ_2 concentration range of 0.01−500 μM. An additional incubation was initiated by the addition of 40 μL of a 5 mM stock solution of 15d-PGJ_2 in reaction buffer (lacking GSH) to 60 μL of 1.7 μM enzyme, giving final concentrations of 2 mM and 1 μM, respectively. After a 1 h incubation on ice,

dx.doi.org/10.1021/bi2019332 | *Biochemistry* 2012, 51, 2348−2356

2.5 μL of a 100 mM stock solution of GSH in 100 mM KH_2PO_4 (pH 7.0) was added to the preincubated protein, mixed, and incubated at 0 °C for 5 min. The reaction was initiated by the addition of 100 μL of each sample to 5 μL of 100 μM PGH_2 in acetone and the mixture incubated at 22 °C for 1 min. Unreacted PGH_2 decomposed to MDA and 12-HHT after the addition of 200 μL of 50 mM $FeCl_2$ in 500 mM KH_2PO_4 (pH 2). To form a fluorescent complex of MDA in solution, 500 μL of 15 mM thiobarbituric acid (TBA) in 80 mM KH_2PO_4 (pH 2.0) was added to the reaction mixture and the mixture heated to 80 °C for 30 min. The precipitate was removed by centrifugation, and the resulting fluorescent MDA−TBA complex was detected with a Horiba Fluorolog fluorescence spectrometer, tuned to excitation and emission wavelengths of 530 and 550 nm, respectively. The same method was used to examine the inhibition of MPGES1 by 11-hydroxy-15d-PGJ_2 and 9-(*S*-glutathionyl)-11-hydroxy-15d-PGJ_2.

Covalent Modification of MPGES1 by 15d-PGJ_2. The site of adduction of the enzyme by 15d-PGJ_2 was determined by LC−MS/MS sequencing. The covalent modification was initiated by the addition of 2 μL of 25 mM 15d-PGJ_2 in dimethyl sulfoxide (DMSO) to 100 μL of 1 mg/mL (60 μM) purified native enzyme in 50 mM KH_2PO_4 (pH 7) containing 300 mM KCl, 7.5% glycerol, 1% CHAPS, and either 1 mM GSH or 1 mM GSO_3^-. After an overnight incubation at 4 °C, the Michael adduct was reduced with $NaBH_3CN$, as described above. For MS analysis, 10 μL of the preincubated protein was diluted 5-fold in H_2O at 22 °C, after which 50 μL of ice-cold 100 mM KH_2PO_4 (pH 2.3) was added, decreasing the pH to 2.5. The protein was then digested on ice for 5 min by the addition of 2 μL of 10 mg/mL (290 μM) pepsin in H_2O. The resulting peptides were separated by HPLC at 0 °C on a Phenomenex Jupiter 5 μm, 300 Å C18 column (50 mm × 1.00 mm) and eluted at 0.3 mL/min with a 30 min gradient from 2 to 50% CH_3CN with 0.4% formic acid. Ions at m/z 300−1500 were detected on a ThermoFinnigan TSQ triple-quadrupole mass spectrometer using positive electrospray ionization. Peptides containing the reduced adduct were identified as those with a mass shift corresponding to the monoisotopic mass of reduced 15d-PGJ_2 and were verified by MS/MS sequencing.

To determine the regiochemistry of enzyme adduction on 15d-PGJ_2, the procedure from the previous paragraph was repeated on a ThermoFinnigan LTQ ion trap mass spectrometer with positive electrospray ionization. The peptide identified as containing the PG adduct was subject to MS^3 fragmentation, selecting for the y ion containing the adducted cysteine 59 residue.

Analysis of Backbone Amide H/D Exchange Kinetics. The methods of the H/D exchange assay and kinetic analysis were performed as previously described.[20,23] The analysis was performed on the native enzyme, as well as the C59A mutant, in complex with either GSH or GSO_3^-, and in the presence of 500 μM 15d-PGJ_2. Preincubation of the enzyme with the inhibitor was initiated by the addition of 4 μL of 25 mM 15d-PGJ_2 in DMSO to 200 μL of 1 mg/mL (60 μM) purified native enzyme or C59A mutant in 50 mM KH_2PO_4 (pH 7.0) containing 300 mM KCl, 7.5% glycerol, 1% CHAPS, and either 1 mM GSH or 1 mM GSO_3^-, and the mixture was incubated overnight at 4 °C. Deuterium incorporation was initiated by a 5-fold dilution of 10 μL of the preincubated protein solution in D_2O at 22 °C. The incorporation was then quenched by a 2-fold dilution in ice-cold 100 mM KH_2PO_4 (pH 2.3). The protein was then digested on ice for 5 min by the addition of 2 μL of 10 mg/mL (290 μM) pepsin in H_2O. The resulting peptides were separated by reversed-phase HPLC at 0 °C on a Phenomenex Jupiter 5 μm, 300 Å, C18 column (50 mm × 1.00 mm) and eluted at a flow rate of 0.3 mL/min with a 15 min gradient from 2 to 50% CH_3CN with 0.4% formic acid. The elution conditions differ from those previously reported[20] to resolve peptide 49−59. However, it was no longer possible to resolve peptide 49−58, a peptide previously utilized to analyze the structural impact of competitive inhibitor binding. Scans from m/z 300 to 1500 were utilized for peptide detection on a ThermoFinnigan TSQ triple-quadrupole mass spectrometer using positive electrospray ionization. Deuterium incorporation was observed as a shift in the centroid of the ion envelope (average mass) for each peptide.

RESULTS

Kinetics of the Spontaneous Reaction of 15d-PGJ_2 with GSH. The spontaneous reaction of GSH with 15d-PGJ_2 (Scheme 1) was previously documented[12] but not with respect to its kinetics. The kinetics of the approach to equilibrium for the reaction at pH 7.0 and 25 °C, determined under pseudo-first-order conditions where [GSH] ≫ [15d-PGJ_2], gave rate constants k_1 (0.75 ± 0.02 M^{-1} s^{-1}) and k_{-1} [(2.0 ± 0.7) × 10^{-4} s^{-1}] for the forward and reverse reactions, respectively. An equilibrium constant for the formation of the adduct can be estimated from $K_f = k_1/k_{-1} \approx 3800 \pm 1000$ M^{-1}. Analysis by HPLC of reaction mixtures of GSH and 15d-PGJ_2 at various concentrations gave a similar K_f value of 1700 ± 200 M^{-1}.

Scheme 1

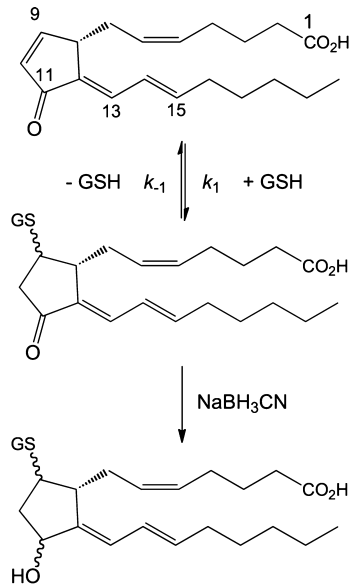

Regiochemistry of the Spontaneous Reaction of 15d-PGJ_2 with GSH and L-Cys. The reaction of 15d-PGJ_2 with GSH or L-Cys resulted in one major peak on analysis by HPLC. Further analysis by LC−MS/MS fragmentation revealed C-9 to be the predominant site of Michael adduction on 15d-PGJ_2 by both GSH and L-Cys, in agreement with what was previously reported for GSH.[12] However, both of these adducts proved to be labile under the ESI conditions in the mass spectrometer. Reduction of the adduct with $NaBH_3CN$ (Scheme 1) provided

dx.doi.org/10.1021/bi2019332 | *Biochemistry* 2012, 51, 2348−2356

a stable product for more definitive analysis by MS/MS (Figure S1 of the Supporting Information). This analysis provided positive evidence for adduction at C-9 but no evidence for adduction at C-13 or C-15. The observation of a single major species by HPLC and the absence of any MS/MS evidence for addition at C-13 or C-15 suggested that the major site of adduction was C-9.

Diastereoselectivity of the Reaction of GSH with 15d-PGJ$_2$. An earlier paper[12] suggested that the stereochemistry of addition of GSH to 15d-PGJ$_2$ occurred on the *si* face (bottom) of the 9−10 double bond, resulting in (9*S*)-*S*-glutathionyl-15d-PGJ$_2$. Our examination of molecular models, however, indicated that the approach of the nucleophile from the *si* face was considerably more hindered and less likely than addition from the top (*re* face). Given that, we revisited the structure of the adduct with high-field NMR spectroscopy.

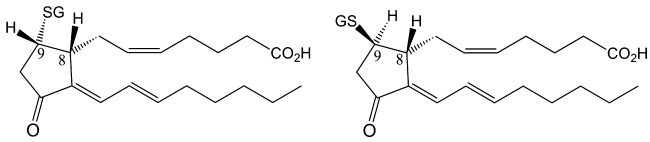

(9*S*)-S-glutathionyl-15d-PGJ$_2$ (9*R*)-S-glutathionyl-15d-PGJ$_2$

A detailed NMR analysis of the purified adduct at 600 and 900 MHz in D_2O and CD_3OD was consistent only with the addition of GSH from the *re* face resulting in the (9*R*)-*S*-glutathionyl-15d-PGJ$_2$ diastereomer. The NMR assignments for this molecule were established using 2D $^1H-^1H$ COSY/DQF-COSY and NOESY along with 2D $^1H-^{13}C$ HSQC experiments. The stereochemistry of the glutathione adduct was determined by analysis of H-7 (2.36, 2.27 ppm), H-8 (3.06 ppm), H-9 (4.57 ppm), and H-10 (2.81, 3.05 ppm). In the 1D NMR spectrum in CD_3OD, H-9 appears as two doublets, which strongly suggests coupling between two protons and not three. These doublets were assigned to coupling between H-9 and the two protons on C-10 and confirmed in the 2D COSY spectrum. The COSY spectrum shows two correlations between H-9 and the two H-10 protons and no correlation between H-9 and H-8. The NOESY spectrum also revealed correlations between the C-10 protons and H-9 but no evidence of a correlation between H-9 and H-8. The lack of a coupling between H-8 and H-9 can be explained if the bond angle between these two protons approaches 90°, which is unique to the (9*R*)-*S*-glutathionyl-15d-PGJ$_2$ diastereomer.

When the solvent was switched to D_2O, changes were observed in the chemical shifts for H-7 (2.41, 2.45 ppm), H-8 (3.17 ppm), H-9 (4.75 ppm), and H-10 (3.03, 3.20 pm). A triplet was observed for H-9 in D_2O, which is again consistent with coupling to two protons (H-10). Results of both 2D COSY and DQF-COSY showed coupling between H-9 and H-10 but no evidence of coupling between H-8 and H-9. This was further supported by the 2D NOESY experiment, which also failed to show any correlation between H-8 and H-9. NMR spectra of 9-GS-15d-PGJ$_2$ are provided in the Supporting Information (Figures S2−S4 and Table S1).

Covalent Modification of MPGES1 by 15d-PGJ$_2$. The original work of Quraishi et al.[19] suggested that the inhibition of MPGES1 by 15d-PGJ$_2$ might be covalent in nature. An examination of the three-dimensional structure of the protein determined by Jegerschöld et al.[24] indicated that there were three buried cysteine residues and one (C49) on the surface. LC−MS/MS sequencing of the native MPGES1 enzyme covalently modified by the 15d-PGJ$_2$ and digested with pepsin revealed that C59 of peptide 49−59 was the specific and exclusive site of PG adduction. An estimate of the ratio of adducted to unadducted peptide suggested that there were ∼0.2 adduct/subunit. When the adduct was stabilized by reduction with $NaBH_3CN$, analysis of the TIC chromatographs of MPGES1 complexed with GSH revealed that approximately 80−90% of the enzyme is modified under the experimental conditions of the H/D exchange assay, while the MPGES1·G-SO_3^- complex appeared to be fully adducted.

The regiochemistry of the protein adduct was determined by MS^3 experiments on the peptic peptide containing C59. The peptide identified as containing the 15d-PGJ$_2$ adduct (residues 49−59) was subjected to MS^3 fragmentation selecting for the y ion of the adducted C59 residue. The results, shown in Figure S5 (Supporting Information), provide evidence of only adduction at C-9 of 15d-PGJ$_2$, as was found with the GSH adduct. However, the absence of evidence for addition at C-13 of C-15 of 15d-PGJ$_2$ does not strictly rule out its occurrence.

Catalytic Properties of MPGES1 and Its C59A Mutant. The catalytic and physical properties of MPGES1 were observed as previously described.[21] The C59A MPGES1 protein exhibited a catalytic activity toward PGH_2 that was indistinguishable from that of the native enzyme. Neither the native enzyme nor the C59A mutant catalyzed the addition of GSH to 15d-PGJ$_2$.

Inhibition of MPGES1 by 15d-PGJ$_2$. The native enzyme was inhibited by 15d-PGJ$_2$ with an IC_{50} value of 0.6 μM (Figure 2A), in good agreement with results previously reported.[19] Inasmuch as the concentration of the enzyme in the assay is ≈1 μM, the value of 0.6 μM is the upper limit of the true IC_{50} and covalent modification is close to complete. Moreover, increasing the substrate concentration failed to rescue the activity of native MPGES1, suggesting that the inhibition was not competitive (Figure 3A). In contrast, the inhibition of the C59A mutant of MPGES1 was reversible with increasing concentrations of PGH_2 (Figure 3B) with an IC_{50} value of 12 μM (Figure 2B). The inhibition of the native enzyme utilizing 11-OH-15d-PGJ$_2$ as an inhibitor was similar to that of the C59A mutant, with IC_{50} values of 11 and 16 μM, respectively (Figure 2). Neither enzyme was appreciably inhibited by 9-(*S*-glutathionyl)-11-hydroxy-15d-PGJ$_2$.

H/D Exchange MS of Native MPGES1 and MPGES1 C59A. The backbone H/D exchange kinetics of the native MPGES1 enzyme, complexed with GSH, in the presence or absence of 15d-PGJ$_2$ were compared. Kinetic plots for some selected peptides are shown in Figure 4. A complete set of kinetic plots for all peptides along with the amplitudes and rate constants for the fits of the data is provided in the Supporting Information (Figures S6−S15). These data reveal that peptides in the proximity of, or containing, residue C59 (peptides 37−54, 49−59, and 60−68) (Figure 5A) displayed decreased deuterium incorporation rates when adducted with 15d-PGJ$_2$. This was not unexpected, inasmuch as 15d-PGJ$_2$ is adducted to C59. In addition to these changes, peptides within the α-helical core of the protein (peptides 78−83, 104−107, 124−129, 130−132, 133−140, and 141−152) also displayed significant differences in H/D exchange behavior (Figures 4C,D and 5A). On further inspection, it was obvious that these regions were similar to those previously identified as constituting the hydrophobic substrate binding cleft by H/D exchange experiments with the MPGES1·GSH complex in the presence of inhibitors competitive for PGH_2 binding.[20]

dx.doi.org/10.1021/bi2019332 | *Biochemistry* 2012, 51, 2348−2356

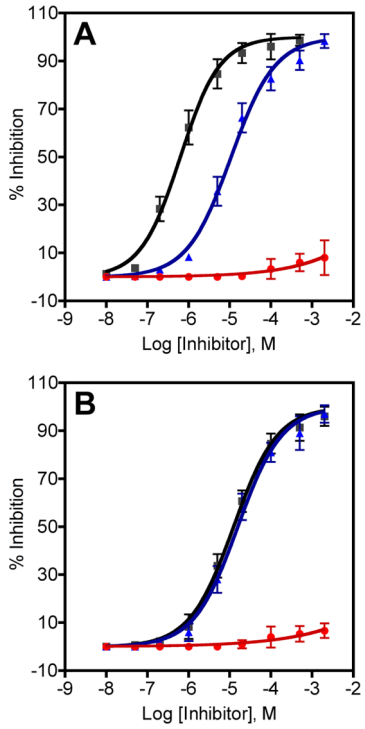

Figure 2. Inhibition of the isomerase activity of native MPGES1 (A) and the C59A mutant (B) by 15d-PGJ_2 (black), 11-OH-15d-PGJ_2 (blue), and 9-GS-11-OH-15d-PGJ_2. The IC_{50} values, 95% confidence range, and Hill coefficients are given in parentheses for MPGES1 (0.6 μM, 0.5–0.8 μM, and 0.91 for 15d-PGJ_2; 11 μM, 9–13 μM, and 0.84 for 11-OH-15d-PGJ_2; and $\gg$1 mM for 9-GS-11-OH-15d-PGJ_2) and for C59A MPGES1 (12 μM, 11–14 μM, and 0.81 for 15d-PGJ_2; 16 μM, 13–19 μM, and 0.79 for 11-OH-15d-PGJ_2; and $\gg$1 mM for 9-GS-11-OH-15d-PGJ_2).

To further explore the possibility that MPGES1 binds 15d-PGJ_2 in its substrate-binding site, the experiments described above were repeated with the MPGES1 C59A mutant. The H/D exchange kinetics of the C59A mutant in complex with GSH are essentially the same as those of the native enzyme as shown in Figure 4. However, the H/D exchange kinetics of MPGES1 C59A in the presence of GSH and 15d-PGJ_2 are remarkably different. Here regions in the proximity of A59 display no significant difference in deuterium incorporation rates. Regions within the CHAPS micelle (residues 18–23, 78–83, 104–107, 124–129, 130–132, 133–140, and 141–152), however, do display changes (Figure 5B), which are associated with the noncovalent binding of 15d-PGJ_2 to the substrate binding site.

To eliminate contributions of the spontaneous adduction of 15d-PGJ_2 to the cofactor, GSH, H/D exchange kinetic analysis of native MPGES1 as well as MPGES1 C59A complexed with GSO_3^- was performed in the absence and presence of 15d-PGJ_2 (Figures 6 and 7). Here, peptide 37–54 (Figure 7A) still displays an overall decrease in deuterium incorporation rates for the native enzyme, whereas peptides 49–59 and 60–68 no longer display this large change in kinetics. This may be due to the fact that GSO_3^- binding distorts the structural conformation of MPGES1,[19] complicating the interpretation of the data. Regions within the detergent micelle (peptides 78–83, 104–107, 130–132, and 141–152) still exhibit substantial changes in H/D exchange kinetics, suggesting that the enzyme binds 15d-PGJ_2 within in the substrate binding site.

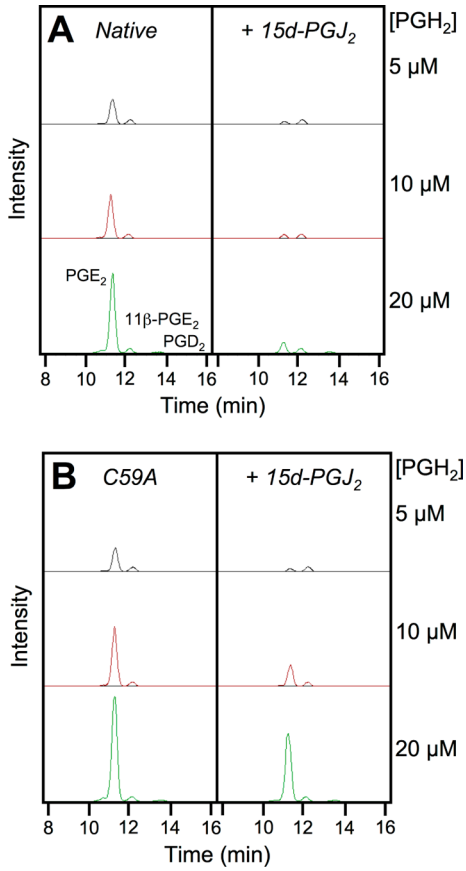

Figure 3. (A) Assay of native and 15d-PGJ_2-modified MPGES1 and (B) the C59A mutant in the absence and presence of 100 μM 15d-PGJ_2, at three different concentrations of the substrate, PGH_2.

DISCUSSION

Chemistry of 15d-PGJ_2. The formation of 15d-PGJ_2 and its reactions with cellular nucleophiles have been studied by

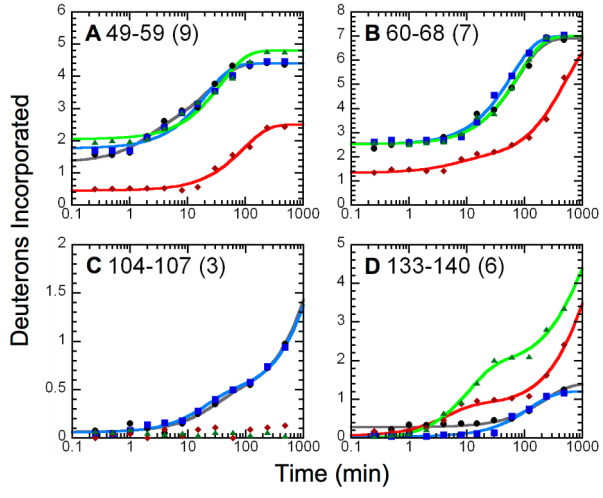

Figure 4. Selected H/D exchange kinetic profiles of native (black) and C59A mutant (blue) MPGES1 in complex with GSH in the absence of 15d-PGJ_2 and the native (red) and C59A mutant (green) enzyme in the presence of 15d-PGJ_2. Data for the GSH and GSO_3^- complexes of the native enzyme (except for peptide 49–59) are from ref 20 and are shown for comparison. The amplitudes and rate constants for the fits of the data can be found in the Supporting Information.

dx.doi.org/10.1021/bi2019332 | *Biochemistry* 2012, 51, 2348–2356

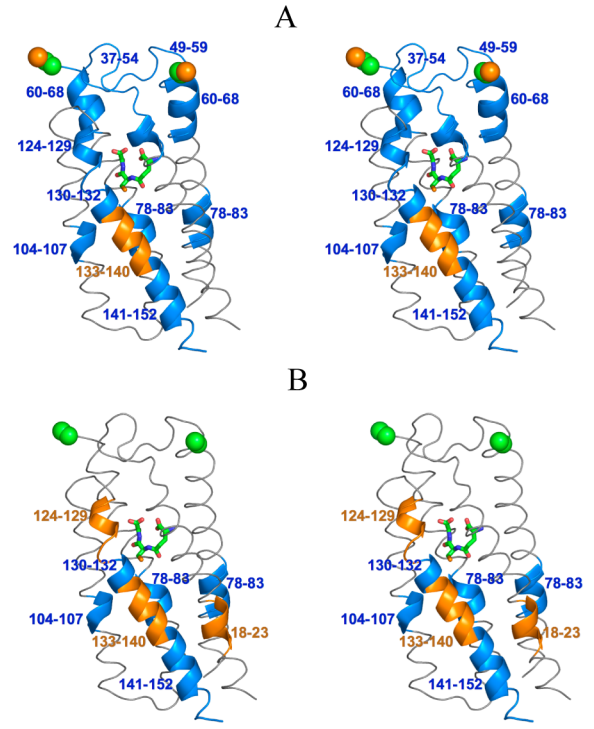

Figure 5. Stereoviews of H/D exchange results mapped to the secondary structural elements in (A) the native protein and (B) the C59A mutant. Representation of the three-dimensional structure of MPGES1 was derived from Protein Data Bank entry 3DWW.[24] A single active site is composed of transmembrane helices Ia and IIa from one subunit and helices IIb, IIIb, and IVb from the adjacent subunit, with GSH shown as sticks. The blue and orange peptides represent regions with decreased and increased rates of exchange, respectively, in the presence of 15d-PGJ_2.

numerous investigators. The regiochemistry of the reaction of GSH with 15d-PGJ_2 appears to occur predominantly at C-9 as

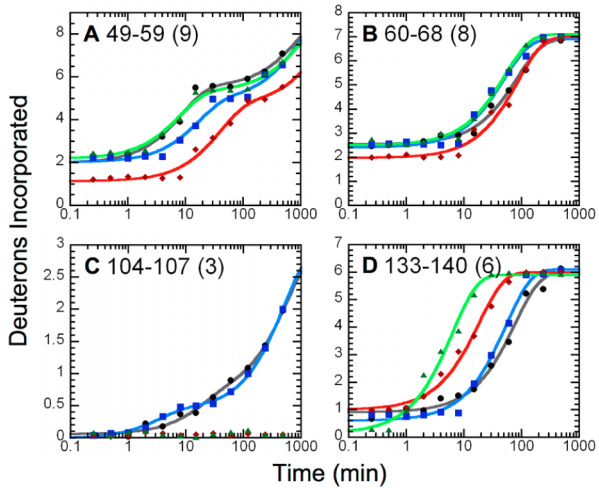

Figure 6. Selected H/D exchange kinetic profiles of native (black) and C59A mutant (blue) MPGES1 in complex with GSO_3^- in the absence of 15d-PGJ_2 as well as the native enzyme (red) and the C59A mutant (green) in the presence of 15d-PGJ_2. Data for the GSH and GSO_3^- complexes of the native enzyme (except for peptide 49−59) are from ref 20 and are shown for comparison. The amplitudes and rate constants for the fits of the data can be found in the Supporting Information.

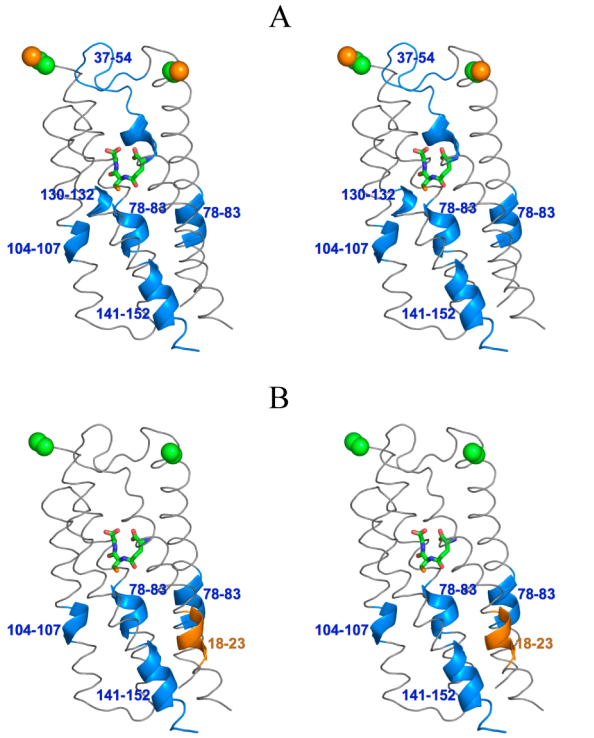

Figure 7. Stereoviews of H/D exchange results mapped to the secondary structural elements in (A) the native protein and (B) the C59A mutant in complex with GSO_3^-, where the position of GSH in the native protein is shown as sticks. The three-dimensional structure of MPGES1 was derived from Protein Data Bank entry 3DWW.[24] A single active site is composed of transmembrane helices Ia and IIa from one subunit and helices IIb, IIIb, and IVb from the adjacent subunit. The blue and orange peptides represent regions with decreased and increased rates of exchange, respectively, in the presence of 15d-PGJ_2.

previously reported by others.[12,25,26] This is also shown to be true for the adduction of MPEGS1 at C59. The stereoselectivity of the spontaneous reaction was reported give the (9*S*)-(*S*-glutathionyl)-15d-PGJ_2 diastereomer.[12] In contrast, our NMR results at 600 and 900 MHz in D_2O and CD_3OD suggest that the nucleophile adds to the least hindered face of the 9−10 double bond to give the (9*R*)-(*S*-glutathionyl)-15d-PGJ_2 diastereomer.

The chemistry and kinetics of the reaction of GSH with 15d-PGJ_2 are key elements in understanding the cellular concentration of the cyclopentenone and its potential anti-inflammatory activity. The spontaneous reaction with GSH is relatively slow (~3 × 10^{-3} s^{-1}) at pH 7, 25 °C, and physiological concentrations of GSH (~4 mM). Once formed, the adduct has a half-life of ~1 h. It is also clear that at chemical equilibrium in an aqueous solution virtually all 15d-PGJ_2 is in the form of the 9-*S*-glutathionyl adduct. The rates of formation of 9-*S*-glutathionyl-15d-PGJ_2 and its penultimate precursor, PGJ_2, are also known to be accelerated, in vitro, by soluble glutathione transferases.[23,26] However, the efficiency of the enzyme-catalyzed addition of GSH, at least to PGJ_2, appears to be rather low with k_{cat}/K_M values of 100−300 M^{-1} s^{-1}.[26] The exact role of GSH transferases in the metabolic disposition of PGJ_2 and 15d-PGJ_2 is not known.

Inhibition of MPGES1 by 15d-PGJ_2. The anti-inflammatory properties of 15d-PGJ_2 may be associated with its inhibition of MPGES1. As defined in this work, there are two

dx.doi.org/10.1021/bi2019332 | *Biochemistry* 2012, 51, 2348−2356

mechanisms of inhibition: the covalent modification of MPGES1 at C59 and the competitive inhibition revealed by the experiments with the C59A mutant. It is also clear that the enzyme is not inhibited by (9*R*)-*S*-glutathionyl-15d-PGJ_2 and that the enzyme does not catalyze the formation of this molecule. It is highly unlikely that a noncovalent, competitive inhibition of MPEGS1 by 15d-PGJ_2 ($IC_{50} \approx 12\ \mu M$) has any biological relevance in vivo. The concentration of free 15d-PGJ_2 in the cell, though unknown, is likely to be well below the micromolar range.[27] The most robust inhibition of the enzyme is via the covalent modification of C59 with an IC_{50} of $\leq 0.6\ \mu M$. It is important to point out that this IC_{50} is an upper limit given the low sensitivity of the inhibition assay.

The effects of the modification of C59 on the H/D exchange behavior of the backbone could suggest a possible physical mechanism for the covalent inhibition of the enzyme. The substrate of MPEGS1, PGH_2, is generated on the luminal side of the membrane, and the product is thought to be released from the cytosol face.[28−30] The exact pathways for entry and egress, however, are not clear. One can imagine entry of the substrate from the luminal face of the enzyme and dissociation of the product from the cytosolic side, or the lateral diffusion of the substrate from the membrane into the active site and the lateral release of PGE_2 into the membrane and subsequent release to the cytosol. The predominant effect of the covalent modification of MPGES1 by 15d-PGJ_2 on the H/D exchange behavior of the backbone is a decreased rate of exchange at the cytosolic ends of helices TMI and TMII and the cytosolic loop that connects them (Figure 5). Cysteine 59 is located at the junction of the cytosolic loop and TMII. If the decrease in H/D exchange rates reflects a reduced flexibility of the egress channel for the product, then the inhibitory effect of the covalent modification of C59 could be reasonably ascribed to blockage of product release.

In contrast, the competitive inhibition of MPEGS1 by noncovalent inhibitors that appear to occupy the substrate binding site often increases the H/D exchange kinetics of the cytosolic loop between TMI and TMII.[20] This observation suggests that the physical mechanism of inhibition by competitive inhibitors and the covalent inhibition by 15d-PGJ_2 are quite different. That is to say, the competitive inhibitors restrict the access of the substrate to the active site, while adduction by 15d-PGJ_2 may decrease the flexibility of the product release channel or alter its conformation, preventing either product formation or release.

Biological Consequences of 15d-PGJ_2. Inasmuch as the concentration of 15d-PGJ_2 in the cell is not known, it is not possible to conclude if the covalent modification of MPEGS1 occurs to any significant extent in vivo. In addition to the cellular concentration of 15d-PGJ_2, there are other issues that are not fully understood. For example, the kinetics and stereochemistry of its reaction with C59 with 15d-PGJ_2 have not been evaluated. Given the physical properties of the molecule, the location of 15d-PGJ_2 is likely to be concentrated in the membrane where the enzyme is also located. Moreover, it is not known if the efficiency of soluble or membrane-bound GSH transferases is sufficient to contribute to the clearance of 15d-PGJ_2 by catalyzing the formation of the GSH adduct.

Although potential biological effects of 15d-PGJ_2 such as those cited in this paper and elsewhere[11] are interesting, the significance of all these findings is complicated by what we do not know. The biological effects of 15d-PGJ_2 formed in vivo are controversial inasmuch as the formation, concentration, location, and metabolic disposition of the molecule are poorly understood.[10] The concentration of 15d-PGJ_2 in human urine has been estimated to be in the low picomolar range, suggesting that its level is insufficient to support biological activity.[27] However, the level in urine may not reflect local cellular concentrations that could greatly affect its bioactivity.

Finally, the transformation of PGD_2 to 15d-PGJ_2 appears to occur by spontaneous chemistry that is unregulated. This fact alone would suggest that 15d-PGJ_2 may not play a regulatory role as an anti-inflammatory molecule. That does not mean, however, that it could not play a role under pathological conditions.

■ CONCLUSIONS

The results reported in this paper demonstrate that 15d-PGJ_2 can act as an effective covalent inhibitor of MPGES1 in vitro and define, from a chemical and physical standpoint, the interaction of the inhibitor with the enzyme. A structure of the adducted enzyme would greatly facilitate our understanding of the physical mechanism of inhibition. The currently available biological data do not preclude an anti-inflammatory role for 15d-PGJ_2 in vivo. However, the gaps in our knowledge of the in vivo concentration of 15d-PGJ_2, its kinetic disposition, and its homeostasis are too large to conclude that it plays a direct role in the biochemistry of inflammation.

■ ASSOCIATED CONTENT

Supporting Information

MS fragmentation analysis of the L-Cys adduct with 15d-PGJ_2 (Figure S1), NMR spectra of 9-(*S*-glutathionyl)-15d-PGJ_2 (Figures S2−S4), chemical shifts and coupling constants from the NMR spectra (Table S1) MS^3 fragmentation of peptide 49−59 from MPGES1 modified with 15d-PGJ_2 (Figure S5), H/D exchange kinetic profiles, including the amplitudes and rate constants for all peptides in MPGES1 and MPGES1 C59A in the presence and absence of 15d-PGJ_2 (Figures S6−S15), and the peptic peptide map of MPGES1 (Figure S16). This material is available free of charge via the Internet at http://pubs.acs.org.

■ AUTHOR INFORMATION

Corresponding Author

*Phone: (615) 343-2920. Fax: (615) 343-2921. E-mail: r.armstrong@vanderbilt.edu.

Funding

This work was supported by National Institutes of Health Grants R01 GM030910 (to R.N.A.), T32 GM008320 (to E.B.P.), and P30 ES000267, the Swedish Research Council. and the Ulla och Gustaf af Ugglas foundation. Support for the 600 and 900 MHz nuclear magnetic resonance spectrometers at Vanderbilt University was provided by grants from the National Institutes of Health (S10 RR019022) and the National Science Foundation (0922862), respectively.

Notes

All authors declare that they have no financial or other conflicts of interest associated with this work.

■ ACKNOWLEDGMENTS

The authors thank Prof. Lawrence Marnett (Vanderbilt University), Dr. Caroline Jegerschöld and Prof. Hans Hebert (Karolinska Institute) for helpful discussions.

■ ABBREVIATIONS

9-GS-15d-PGJ$_2$, 9-(*S*-glutathionyl)-15-deoxy-$\Delta^{12,14}$-prostaglandin J$_2$; 9-GS-11-OH-15d-PGJ$_2$, 9-(*S*-glutathionyl)-11-hydroxy-15-deoxy-$\Delta^{12,14}$-prostaglandin J$_2$; 11-OH-15d-PGJ$_2$, 11-hydroxy-15-deoxy-$\Delta^{12,14}$-prostaglandin J$_2$; 12-HHT, 12(*S*)-hydroxy-8,10-*trans*-5-*cis*-heptadecatrienoic acid; 15d-PGJ$_2$, 15-deoxy-$\Delta^{12,14}$-prostaglandin J$_2$; CHAPS, 3-[(3-cholamidopropyl)dimethylammonio]-1-propanesulfonate; COX, cyclooxygenase; coxib, COX-2 selective inhibitor; cyPG, cyclopentenone prostaglandin; DEAE, diethylaminoethyl weak anion exchange; DMSO, dimethyl sulfoxide; DP, D-prostanoid receptor; DTT, dithiothreitol; EP, E-prostanoid receptor; GSH, glutathione; GSO_3^-, glutathione sulfonate; H/D, hydrogen/deuterium; MDA, malondialdehyde; MPGES1, microsomal prostaglandin E synthase 1; MS, mass spectrometry; NSAID, nonsteroidal anti-inflammatory drug; PG, prostaglandin; PPARγ, peroxisome proliferator-activated receptor γ; SRM, single-reaction monitoring; TBA, thiobarbituric acid.

■ REFERENCES

(1) Willis, A. L., and Cornelsen, M. (1973) Repeated injection of prostaglandin E$_2$ in rat paws induces chronic swelling and a marked decrease in pain threshold. *Prostaglandins 3*, 353−357.

(2) Jackson, G. M., Sharm, H. T., and Varner, M. W. (1994) Cervical ripening before induction of labor: A randomized trial of prostaglandin E$_2$ gel versus low-dose oxytocin. *Am. J. Obstet. Gynecol. 171*, 1092−1096.

(3) Robert, A., Shultz, J. R., Nezamis, J. E., and Lancaster, C. (1976) Gastric antisecretory and antiulcer properties of PGE$_2$, 15-methyl PGE$_2$, and 16,16-dimethyl PGE$_2$. Intravenous, oral and intrajunal administration. *Gastroenterology 70*, 359−370.

(4) Arvind, P., Papavassiliou, E. D., Tsioulias, G. J., Qiao, L., Lovelace, C. I. P., Duceman, B., and Rigas, B. (1995) Prostaglandin E$_2$ down-regulates the expression of HLA-DR antigen in human colon adenocarcinoma cell lines. *Biochemistry 34*, 5604−5609.

(5) Roberts, L. J., and Sweetman, B. J. (1985) Metabolic fate of endogenously synthesized prostaglandin D$_2$ in human female with mastocytosis. *Prostaglandins 30*, 383−400.

(6) Hyaishi, O. (1988) Sleep-wake regulation by prostaglandins D$_2$ and E$_2$. *J. Biol. Chem. 263*, 14593−14596.

(7) Onoe, H., Ueno, R., Fujita, I., Nishino, H., Oomura, Y., and Hayaishi, O. (1988) Prostaglandin D$_2$: A cerebral sleep-inducing substance in monkeys. *Proc. Natl. Acad. Sci. U.S.A. 85*, 4082−4086.

(8) Straus, D. S., and Glass, C. K. (2001) Cyclopentenone prostaglandins: New insights on biological activities and cellular targets. *Med. Res. Rev. 21*, 185−210.

(9) Fitzpatrick, F. A., and Wynalda, M. A. (1983) Albumin-catalyzed metabolism of prostaglandin D$_2$: Identification of products formed in vitro. *J. Biol. Chem. 258*, 11713−11718.

(10) Powell, W. S. (2003) 15-Deoxy-$\Delta^{12,14}$-PGJ$_2$: Endogenous PPARγ ligand or minor eicosanoid degradation product? *J. Clin. Invest. 112*, 828−830.

(11) Milne, G. L., Yin, H., Hardy, K. D., Davies, S. S., and Roberts, L. J. II (2011) Isoprostane Generation and Function. *Chem. Rev. 111*, 5973−5996.

(12) Paumi, C. M., Wright, M., Townsend, A. J., and Morrow, C. S. (2003) Multidrug resistance protein (MRP) 1 and MRP3 attenuate cytotoxic and transactivating effects of the cyclopentenone prostaglandin, 15-deoxy-$\Delta^{12,14}$-prostaglandin J$_2$ in MCF7 breast cancer cells. *Biochemistry 42*, 5429−5437.

(13) Kim, E. H., and Surh, Y. J. (2006) 15-Deoxy-$\Delta^{12,14}$-prostaglandin J$_2$ as a potential endogenous regulator of redox-sensitive transcription factors. *Biochem. Pharmacol. 72*, 1516−1528.

(14) Stamatakis, K., and Perez-Sala, D. (2006) Prostanoids with cyclopentenone structure as tools for the characterization of electrophilic lipid-protein interactomes. *Ann. N.Y. Acad. Sci. 1091*, 548−570.

(15) Jakobsson, P. J., Thoren, S., Morgenstern, R., and Samuelsson, B. (1999) Identification of human prostaglandin E synthase: A microsomal glutathione-dependent, inducible enzyme, constituting a potential drug target. *Proc. Natl. Acad. Sci. U.S.A. 96*, 7220−7225.

(16) Marnett, L. J. (2009) The COXIB experience: A look in the rearview mirror. *Annu. Rev. Pharmacol. Toxicol. 49*, 265−290.

(17) Samuelsson, B., Morgenstern, R., and Jakobsson, P. J. (2007) Membrane prostaglandin E synthase-1: A novel therapeutic target. *Pharmacol. Rev. 59*, 207−224.

(18) Thorén, S., and Jakobsson, P. J. (2000) Coordinate up- and down-regulation of glutathione-dependent prostaglandin E synthase and cyclooxygenase-2 in A549 cells: Inhibition by NS-398 and leukotriene C4. *Eur. J. Biochem. 267*, 6428−6434.

(19) Quraishi, O., Mancini, J. A., and Riendeau, D. (2002) Inhibition of inducible prostaglandin E$_2$ synthase by 15-deoxy-$\Delta^{12,14}$-prostaglandin J$_2$ and polyunsaturated fatty acids. *Biochem. Pharmacol. 63*, 1183−1189.

(20) Prage, E. B., Pawelzik, S. C., Busenlehner, L. S., Kwangho, K., Jakobsson, P. J., Morgenstern, R., and Armstrong, R. N. (2011) Location of inhibitor binding sites in the human inducible PGE$_2$ synthase MPGES1. *Biochemistry 50*, 7684−7693.

(21) Murphey, L. J., Williams, M. K., Sanchez, S. C., Looretta, M. B., Csiki, I., Oates, J. A., Johnson, D. H., and Morrow, J. D. (2004) Quantification of the major urinary metabolite of PGE$_2$ by a liquid chromatographic/mass spectrometric assay: Determination of cyclooxygenase-specific PGE$_2$ synthesis in healthy humans and those with lung cancer. *Anal. Biochem. 334*, 266−275.

(22) Pawelzik, S. C., Uda, N. R., Spahiu, L., Jegerschold, C., Stenberg, P., Hebert, H., Morgenstern, R., and Jakobsson, P. J. (2010) Identification of key residues determining species differences in inhibitor binding of microsomal prostaglandin E synthase-1. *J. Biol. Chem. 285*, 29254−29261.

(23) Busenlehner, L. S., Codreanu, S. G., Holm, P. J., Bhakat, P., Hebert, H., Morgenstern, R., and Armstrong, R. N. (2004) Stress sensor triggers conformational response of the integral membrane protein MGST1. *Biochemistry 43*, 11145−11152.

(24) Jegerschöld, C., Pawelzik, S. C., Purhonen, P., Bhakat, P., Gheorghe, K. R., Gyobu, N., Mitsuoka, K., Morgenstern, R., Jakobsson, P. J., and Hebert, H. (2008) Structural basis for induced formation of the inflammatory mediator prostaglandin E$_2$. *Proc. Natl. Acad. Sci. U.S.A. 105*, 11110−11115.

(25) Brunoldi, E. M., Zanoni, G., Vidari, G., Sasi, S., Freeman, M. L., Milne, G. L., and Morrow, J. D. (2007) Cyclopentenone prostaglandin, 15-deoxy-$\Delta^{12,14}$-PGJ$_2$, is metabolized by HepG2 cells via conjugation with glutathione. *Chem. Res. Toxicol. 20*, 1528−1535.

(26) Bogaards, J. J. P., Venekamp, J. C., and van Bladeren, P. J. (1997) Stereoselective conjugation of prostaglandin A$_2$ and prostaglandin J$_2$ with glutathione, catalyzed by the human glutathione S-transferases A1-1, A2-2, M1a-1a and P1-1. *Chem. Res. Toxicol. 10*, 310−317.

(27) Bell-Parikh, L. C., Ide, T., Lawson, J. A., McNamara, P., Reilly, M., and FitzGerald, G. A. (2003) Biosynthesis of 15-deoxy-$\Delta^{12,14}$-PGJ2 and the ligation of PPARγ. *J. Clin. Invest. 112*, 954−955.

(28) Lazarus, M., Kubata, B. K., Eguchi, N., Fujitani, Y., Urade, Y., and Hayaishi, O. (2002) Biochemical characterization of mouse microsomal prostaglandin E synthase-1 and its colocalization with cyclooxygenase-2 in peritoneal macrophages. *Arch. Biochem. Biophys. 397*, 336−341.

(29) Bergstrom, S., and Samuelsson, B. (1968) The prostaglandins. *Endeavour 27*, 109−113.

(30) Smith, W. L. (1989) The eicosanoids and their biochemical mechanisms of action. *Biochem. J. 259*, 315−324.